

Journal of Materials Chemistry C

Accepted Manuscript



This is an *Accepted Manuscript*, which has been through the Royal Society of Chemistry peer review process and has been accepted for publication.

Accepted Manuscripts are published online shortly after acceptance, before technical editing, formatting and proof reading. Using this free service, authors can make their results available to the community, in citable form, before we publish the edited article. We will replace this *Accepted Manuscript* with the edited and formatted *Advance Article* as soon as it is available.

You can find more information about *Accepted Manuscripts* in the [Information for Authors](#).

Please note that technical editing may introduce minor changes to the text and/or graphics, which may alter content. The journal's standard [Terms & Conditions](#) and the [Ethical guidelines](#) still apply. In no event shall the Royal Society of Chemistry be held responsible for any errors or omissions in this *Accepted Manuscript* or any consequences arising from the use of any information it contains.

Electrically Responsive Photonic Crystals: a Review

Luca Nucara,^{*a,b} Francesco Greco^{*b} and Virgilio Mattoli^{*b}

DOI: 10.1039/b000000x [DO NOT ALTER/DELETE THIS TEXT]

5 Tunable photonic crystals (TPCs) represent an important class of intelligent materials, which can be used as optically active components and as functional technology to change an object colour. Among these smart structures, electrically responsive photonic crystals are the most promising for real technological applications. Up to now, to transform the electrical
10 stimulus into an optical response several strategies have been adopted that can be classified in 1) electrochemical processes, 2) reorientation of liquid crystal molecules, 3) electrophoretic organization of colloidal suspension and 4) indirect electrically induced modification of the photonic structures. In this review article, these approaches are systematically summarized and
15 analysed with particular emphasis on the chemistry of materials.

1 Introduction

Photonic crystals (PCs) are constituted of alternating regions of materials with different refractive indices arranged in a periodic structure with lattice parameters comparable to the light wavelength of interest. The periodic spatial modulations of
20 the refractive index create forbidden regions, called band gaps or stop-bands, which prevent the propagation of photons with certain energies. As a consequence of the photonic band gaps (PBGs), photonic crystals reflect the incident light at certain frequencies and angles, in dependence on the specific spatial arrangement of materials along one or more principal axes in one-, two- or three-dimensional
25 periodic structures.¹ The bandwidth and the frequency of the PBG are determined by the refractive index contrast between the two materials, the structural symmetry and lattice parameters.

Multilayer systems or 1D-PCs, usually referred to as Bragg reflectors, are the simplest photonic structures and consist of a stack of layered materials with different
30 refractive indices. When material columns are arranged in an in-plane crystal structure, 2D-PCs result. In 3D-PCs instead, materials are arranged according to a three dimensional lattice structure and they are potentially able to totally prevent light propagation within a specific wavelength range and along any direction of PCs by the so called complete PBG. A basic view of different arrangements of PCs is
35 given in Fig. 1a. A particular type of 3D-PC is constituted by opals that result by spherical nanoparticles arranged into ordered arrays and inverted opals, which consist in the negative replica structures of opals.

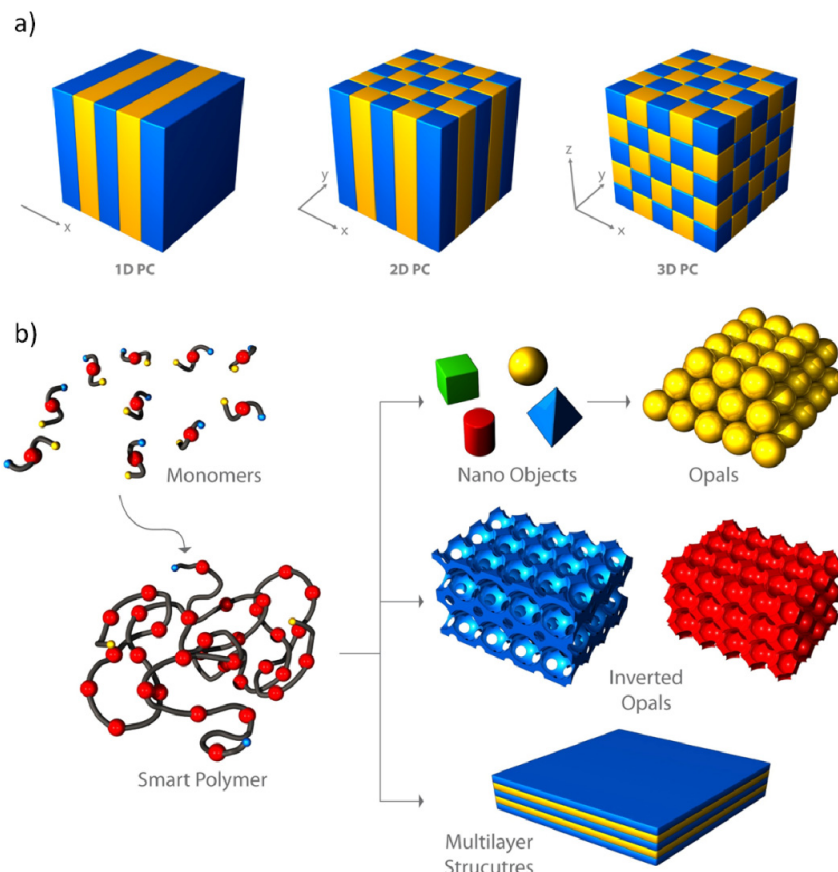


Fig. 1 a) Schematic representation of 1D, 2D and 3D photonic crystals. This classification is determined by the spatial arrangement of the two materials with different refractive indices. b) Schematic outline of the incorporation process of smart polymers into photonic structure. Stimuli responsive polymers can be processed to obtain nano-objects to produce 2D and 3D-PCs, nanostructured matrices or multi-layered architectures as 1D-PCs.

In contrast to the common coloured materials, in which colours are generated from the presence of dyes, colours of PCs are a consequence of their micro- and nanostructure, selectively reflecting a specific wavelength range of the incident light. This mechanism is the basis of structural colours widely found in Nature, as in the case of plants and of several animals, including insects and mollusks.^{2,3} In terms of wavelength, the colour exhibited by photonic crystals can be described by a combination of Bragg's law with Snell's law:⁴

15

$$\lambda_{max} = \frac{2}{m} d \sqrt{n_{eff}^2 - \sin^2 \theta} \quad (1)$$

where λ_{max} is the wavelength at which maximum reflection occurs, m is the order of

Bragg diffraction, d is the lattice constant, n_{eff} is the effective refractive index of the crystal and θ is the angle of incidence with respect to the plane of the photonic crystal. n_{eff} is defined as the weighted sum of the refractive indices of the materials that constitute the crystal:

5

$$n_{eff}^2 = \sum n_i^2 \varphi_i$$

where n_i and φ_i are the refractive index and the volume fraction of each i portion, respectively. This simple formulation provides a description of the scattering properties of the periodic structure in the form of sets of pairs (wavelength and
10 direction) for which the light is diffracted rather than transmitted.

In the simplest case of 1D periodic variation of the dielectric function, the solution of a scalar wave equation leads to an expression for the wavevector as a function of the energy.⁵ For certain energy ranges no purely real solutions exist and the wavevector has a non-vanishing imaginary part. As a consequence, with the
15 approximation of infinite crystal, the wave suffers attenuation and does not propagate. This happens exactly at the wavevector predicted by Bragg's law and for this wavevector there are two solutions in terms of energies that delimit the stop band. The width of the PBG is mainly determined by the dielectric contrast between the two materials constituting the photonic structure.

20 For a more rigorous treatment, it is necessary to keep into account the vectorial character of the electromagnetic radiation. In particular, if the spatial dependence of the relative permittivity of the medium $\varepsilon(\mathbf{r})$ corresponds to that of the periodic lattice, the electromagnetic wave equation for the magnetic field **H**

25

$$\nabla \times \left[\frac{1}{\varepsilon(\mathbf{r})} \nabla \times \mathbf{H}(\mathbf{r}) \right] = \left(\frac{\omega}{c} \right)^2 \mathbf{H}(\mathbf{r}) \quad (2)$$

that is an Hermitian eigenvalue problem, provides the photonic bands (eigenvalues) as series of functions $\omega_n(\mathbf{k})$, where n refers to the band index and \mathbf{k} to the Bloch's wavevector. The dispersion relation determines all the light transport and emission
30 properties of the PCs. More detailed derivation of the band structure and its implications on the optical properties could be found elsewhere.^{1,5-7}

From an applicative point of view, the capability of PCs to interact and to control light propagation renders them interesting for many technological fields; both academic and industrial research has focused on their application in
35 optoelectronics,^{6,8} (optical circuits, lasers and spectroscopy), as high-density magnetic and optical data recording materials,⁹⁻¹¹ displays,¹²⁻¹⁴ sensors,¹⁵⁻¹⁷ colour-changing paints and inks,¹⁸ photonic papers,¹⁹ as well as in medicine.²⁰

Since the concept of PCs has been first proposed by Eli Yablonovitch in 1980s,²¹ several procedures for preparing these materials have been explored, the choice
40 depending on the desired geometry and the periodic arrangement of the materials, which determine the photonic properties of interest for the target application. Basically, a photonic crystal can be realized by microfabrication methods (photolithography, materials deposition and etching techniques) to produce microstructures with desired shape, order level from bulk materials, or by self-
45 assembling of preformed buildings blocks (nano-objects or block copolymers) into periodically structured assemblies.²² Actually, the latter is the most used method,

because of improved efficiency, speed, cost-effectiveness, high throughput on large areas with respect to micro-fabrication.

In the last ten years the main research interest has been focused, not only on theoretical studies of light-matter interactions and on experimental methods to fabricate high-order PCs on large scale, but also on procedures to create PCs whose properties could be tuned by external stimuli. In fact, tunable photonic crystals (TPCs) can be applied as intelligent devices, both as components in optically active based systems (e.g. colour displays, biological and chemical sensors) and as functional material to change an object colour. On the basis of the latter application, once appropriately embedded in an object, TPCs allow changing its colour and modifying its appearances in a controlled way. This application would be particularly attractive when inserting TPCs in an object of daily use, as in the case for example of mobile phones, watches, clothes or shoes. Think, for instance, to a t-shirt which can change its colour with voice or a car's colour which can be switched by simply pushing a button. Other examples regard the possibility to create military suits that are able to modify their colour and to blend according to the surrounding environment for camouflage or furnishings able to vary their look during the day.

The fabrication of stimuli-responsive photonic crystals can be realized in several manners by triggering the change of the parameters that appear in equation (1), such as the lattice constant d or the effective refractive index n_{eff} of the crystal, although other strategies can be adopted.²³ Up to now, literature reports a large number of examples related to tunable photonic crystals, using several external stimuli as a trigger, such as chemical,^{16,24,25} thermal,^{26–28} electrical, magnetic,^{29–31} mechanical^{32,33} stimuli or light.^{34–36} The choice of a stimulus is determined by the specific technological application the PC is targeted to. In fact, for example, the development of an optical gas sensor requires a chemically responsive PC; on the other hand, a PC sensible to temperature variations is necessary in the case of thermal analysis implementation.

Usually, the active material that is able to respond to external stimuli is a polymer. In fact, the chemical and physical properties of the polymers can be finely tailored according to the requirements, by changing the structure of monomers and the synthetic procedure. The smart materials can be embedded into the photonic structures as nanoobjects^{28,37–40} in the case of 2D and 3D-PCs or, in the case of opals and inverted opals, as nanostructured matrices.^{41,42} Otherwise, it is possible to use these materials in multilayer architectures as in the case of 1D-PC.^{43–45} (Fig. 1b)

In general, the responsiveness of a TPC can be evaluated in terms of: (a) band gap tunability range, which can be defined as the wavelength interval of the electromagnetic spectrum inside of which the PBG can be shifted by applying the stimulus; (b) response time, that is the time needed to obtain a stable variation of the PBG with respect to the initial value; (c) refresh time, which is the time to recover the initial value of the PBG. From a practical point of view, it is desirable to develop a technology based on TPCs which allows to finely control the position and the intensity of the reflected wavelength range in a reversible and fast way. In general, problems that can be encountered in the control of the optical properties of TPCs concern the restricted range of obtainable changes of the crystal structure or refractive index. In addition, it is challenging to fabricate architectures with a complete PBG in the visible range.⁴⁶ This is due to the limited choices of transparent materials having high refractive indices, necessary for achieving high refractive index contrast. It is simpler, instead, by using combination of materials with lower

contrast, to produce incomplete or pseudo-PBG materials in the visible range (called iridescent materials) whose colours vary with the viewing angle. Regarding the response speed, TPCs based on chemical or thermal stimulations have often large response time due to the intrinsic slowness of physical or chemical changes that external stimuli may cause. This behaviour is encountered for example in the case of chemically responsive PCs, whose response mechanism's kinetics depend on the diffusion processes of chemical species inside the smart material and can be very slow.¹⁵

In this context, electrically responsive PCs represent one of the most promising tunable PBG materials for technological applications. In fact, electrical stimulus can be finely and easily controlled in a continuous way. Moreover, its implementation is convenient and is usually characterized by a fast response rate. It can be controlled remotely by computer and, by means of micro-fabricated electrodes or metallic lines, electrically responsive systems can be addressed at the microscale, which makes suitable their integration in devices as patternable pixels.

These features can open the way to a new generation of display units for many applications that require presentation of visual information. In fact, PCs are able to generate not photo-bleachable brilliant colours with characteristics that cannot be reproduced by traditional pigments and dyes. Furthermore, a single tunable photonic structure may produce a wide range of colours. Such electrically tunable technology could constitute a real revolution for outdoor usage such as signage and billboard advertising, where most emissive display technology (e.g. liquid crystals, light emitting diode and plasma) are little convenient from the point of view of high production cost and energy consumption. In addition, it would be possible to solve the annoying dazzle in sunshine that the current display technologies suffer. Other applications of these intelligent materials can regard the production of colour pixel in digital photographs, printing and coloured claddings for a variety of objects. In the last few years several excellent reviews have appeared dealing with responsive photonic crystals.^{4,23,42,47,48} Nonetheless a specific review regarding the electrically TPCs, following the recent progresses in this field, is lacking. The aim of this review article is therefore to provide a general and comprehensive treatment of the subject of electrically TPCs, illustrating with a systematic approach the strategies applied to create an optical response to electrical stimulus in these attractive intelligent systems, as well as their limitations and possible future technological applications.

35

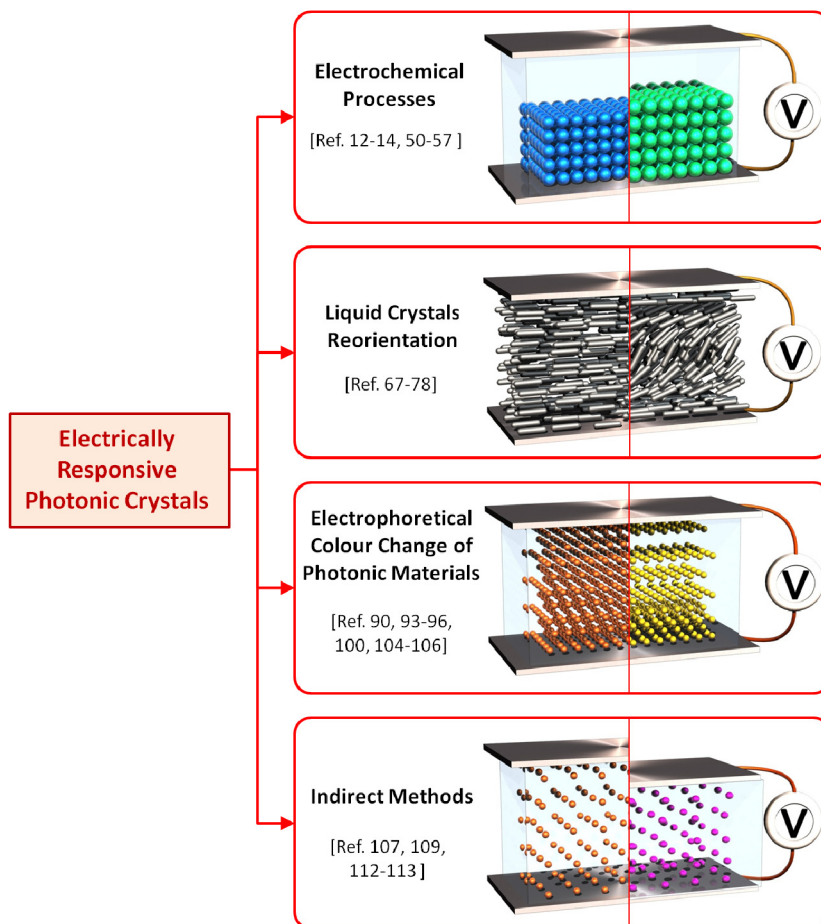


Fig. 2 Schematic outline of the applied strategies for electrically tunable photonic crystal implementation.

The strategies reported in literature that are used for the implementation of electrically TPCs are outlined in Fig. 2 and can be divided in the following categories, depending on the action performed by the electric field: 1) electrochemical process, in which oxidation and reduction modify the photonic structure; 2) reorientation of liquid crystal molecules, to modify the refractive index; 3) electrophoretic organization of colloidal suspension and 4) indirect electrically induced modification of the photonic system.

2 TPCs based on Electrochemical Processes

This type of TPCs is constituted of an electrochemical cell in which an electrochemically responsive material is immersed in a conductive solution. To obtain an electrochemically responsive system it is necessary to include chemical species that can undergo reversible ionization changes, through oxidation-reduction

processes or acid-base exchanges.

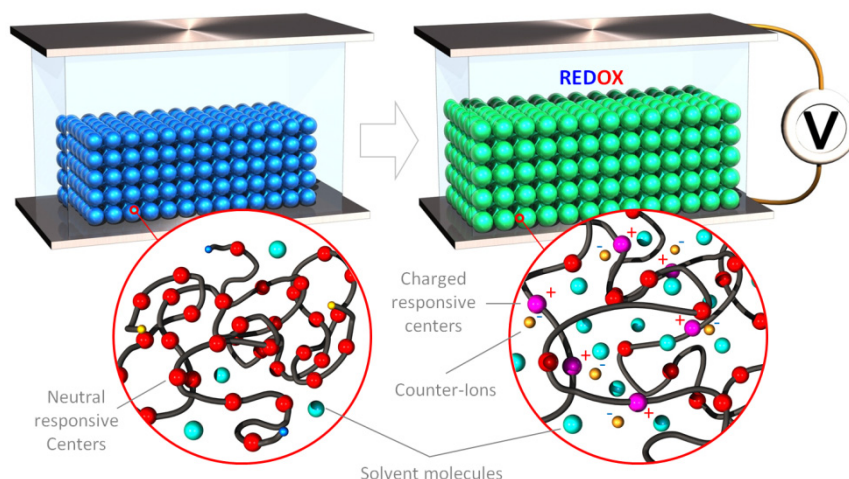


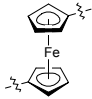
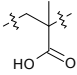
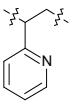
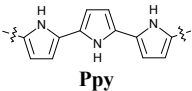
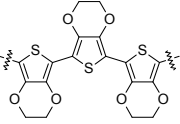
Fig. 3 Schematic outline of working mechanism of TPCs based on electrochemical processes. The applied voltage induces a charge variation on the smart polymer's active sites, causing a swelling of the photonic structure and a red-shift of the reflected wavelength range.

Electric field, in fact, can act directly on the active moieties, by changing their oxidation states, or promote acid-base dissociations, by electrolytic processes. Independently by the activation mechanism, the electrical stimulus induces a localized charge variation in the responsive centers, destabilising the original structure due to electrostatic repulsions (Fig. 3). As a consequence, in order to minimize the repulsive forces between the localized charges, the system undergoes to a structural reorganization, which depends on how electro-active groups are embedded in the photonic structure. The design of an electro-active polymer network usually involves incorporation of electro-responsive moieties in the polymer main chain, in the side groups or as cross-linkers.⁴⁹ Under the application of an electric field, the active sites of the polymeric structure undergo to ionization process depending on the value of the applied voltage; thus, due to repulsive forces between the charged groups, polymer matrix swelling is obtained. As a consequence, solvent molecules can enter inside the polymeric structure, driven by the electrostatic interactions with the sites. This process produces an overall change of the polymer refractive index, as well as a change of its thickness. If the polymer has a spatial periodic nanostructured arrangement, a variation of the lattice constant is obtained, which results, at the end, in a shift of the PBG and then of its colour.

This approach requires the presence of an appropriate conductive solution to ensure a fast migration of electrons, ions and solvent molecules. The solution conductivity actually determines the response speed of the system and the possibility to induce an electrical stimulation with low voltages. Another important aspect to consider is the switching time of the system, which is correlated with the matrix porosity and the affinity of the used solvent with the polymer. Each factor that facilitates the solvent permeation into the polymer decreases the process switching time.

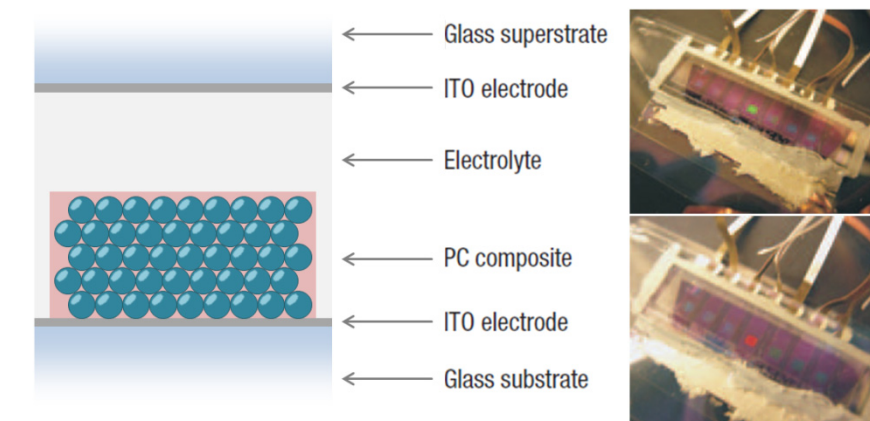
Several examples of electrochemical TPCs and their main properties are summarized in Table 1.

Table 1 Examples of active sites contained in smart polymers for electrochemical tuning of PCs. For each polymer, several performances of the corresponding TPC are summarized.

Material Electro-Active Sites	PBG Shift Range	Applied Voltage	Switching Time	Reversibility	Ref.
 PFS	~ 510 – 610 nm	0.0 – 3.0 V	1-2 s	y	12
	~ 440 – 700 nm	0.0 – 2.8 V	> 4 s	y	50
 PMAA	580 nm ; 800 nm	1.8 V	Several minutes	y	51
 PVP	500 – 675 nm	up to 10 V	Few seconds	y	52
	430 – 650 nm	0.0 – 2.5 V	Several minutes	y	13
	526 – 610 nm	0 – 5 V	~ 3 s	y	14
	486 – 664 nm	-4.5 to -3.5 V 2.0 to 2.4 V	~ 1 s	y	53
 Ppy	576 – 626 nm	0.8 V	16 min	y	54
 PEDOT	574 – 583 nm	-0.8 to 1.3 V	Up to ~ 830 min	y	55,56

The first example of tunable photonic crystals using electrochemical processes was reported by Ozin and Manners,⁵⁷ who demonstrated the possibility to tune the optical stop-band of a colloidal photonic crystal, in terms of position, width and intensity, by electrochemically induced anisotropic expansion/contraction of photonic lattice. The photonic structure was prepared by photo-polymerization of a mixture of (ethyl-methyl)sila-[1]-ferrocenophane and sila(cyclobutyl)-[1]-ferrocenophane infiltrated into a self-assembled colloidal crystal of silica nanoparticles. The resulting cross-linked polyferrocenylsilane (PFS) network shown a continuous variable degree of oxidation, thanks to the ferrocene groups. Because charges on the individual iron atoms in each repeat unit can be controlled between a

0 and +1 state, PFS matrix can have continuous variable interactions with any solvent it contacts. Besides to the very fast and reversible variation of the stop-band under swelling, when these polymer/silica composites were subjected to multiple partial oxidations using a solution of tris(4-bromophenyl)ammonium hexafluorophosphate in dichloromethane (DCM) a decreasing of the reflected wavelength in the swollen state with increasing the degree of oxidation was observed, because the in the oxidized state cannot be efficiently solvated by a non-polar solvent.



10 **Fig. 4** Scheme of electrochemical cell construction of polyferrocenylsilane (PFS) based opal. Photographs of the prototype pixel are also reported. Adapted from ref. 12 with permission of Nature Publishing Group.

15 After reduction by treatment with a solution of decamethylferrocene in DCM, a transmission spectrum almost identical to that in the same solvent before oxidation was obtained, demonstrating the reversibility of the process and thus the suitability of this approach in electrically TPCs.

Subsequently, the same authors reported an impressive upgrade of this technology
 20 by fabricating electrically tunable displays based on PCs, using a mixture of a low molecular weight PFS with pendant unsaturated C=C bonds, a small amount of a multifunctional thiol and a radical photoinitiator (Fig.4).¹² When an oxidative potential is applied to the photonic crystal, iron atoms pass from 0 to +1 oxidation state, making the PFS network electropositive. Consequently, negative ions from the
 25 electrolyte are driven into the polymer to neutralize its positive charges, together with them solvent molecules. In this way, a swelling of the matrix and thus an increase of the distance between silica nanoparticles were observed which correspond to a red-shift of the diffracted light. On the contrary, if a reducing potential is applied, the positive iron ions are reduced with the contemporary
 30 expulsion of anions with their solvent shell, producing an overall contraction of the photonic lattice and then a blue-shift of the diffracted light. In this way, a shift of the reflected peak position from blue to red is achieved upon applying a voltage up to 3 V. Although the peak shift speed is not very high (peak shift occurs within 1-2 s), the process is reversible and stable: the system performances are maintained in a
 35 series of 100 oxidation-reduction cycles, in which the wavelength of peak maximum

shifts reversibly within nanometres after each voltage application.

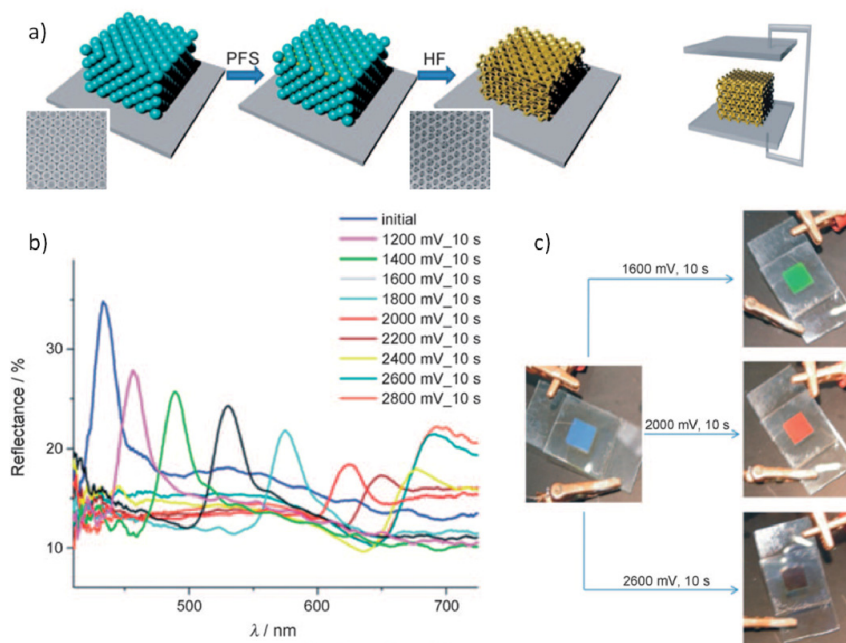


Fig. 5 Full-colour tuning of inverse opals by electrochemical process. a) Schematic outline of the preparation of electrochemical cell based on polyferrocenylsilane (PFS) inverse opal. b) Dependence of reflective spectra of inverse opal on the applied electrical potential. c) Photographs of the cell. Adapted from ref. 50 with permission of Wiley VCH.

A further improvement of this approach was implemented by fabricating an inverse opal structure in which electrolyte solution freely infuses the nanoporous lattice.⁵⁰ In this way it was possible to obtain a complete tunability of the wavelength and brightness of Bragg diffracted light in a continuous fashion all over the visible spectrum, from the ultraviolet to the near infrared, although the wavelength switching time resulted higher than in the case of previous device (Fig 5). By using this porous matrix, significantly enhanced electron and ion transport were observed, allowing to reduce the voltage that is needed to drive the device, together with very good voltage-dependent continuous shifts in reflected light with voltage in the range of 1.2 – 2.8 V. In particular, under an applied bias of 2.8 V, it was possible to shift the photonic stop band of about 250 nm. These exciting performances were attributed to the highly porous structure which improves the specific surface area of the film in contact with the electrolyte solution and simplifies the diffusion of electrons and ions throughout the polymeric matrix.

Based on the same approach, Watanabe and Takeoka presented a porous electrolyte hydrogel of poly(NIPAm-co-MAA) that exhibits switchable colours over the visible spectrum, induced by both electrochemical process and temperature change.⁵¹ This hydrogel undergoes different equilibrium degrees of swelling in response to pH as well as temperature. In particular, when carboxylic groups are ionized to carboxylate, an electrostatic repulsion is produced between the charged

sites in the hydrogel, determining the expansion and swelling of the polymeric network. The authors proposed an inverse opal structure with this polymeric matrix, whose stop-band can be tuned by electrical stimulus in the electrolysis process. In fact, because electrolysis of water causes a change in the pH of an electrolyte solution, the swelling degree of a pH-sensitive hydrogel that is placed on the electrodes can be easily and drastically changed by electrolysis. When a voltage of 1.8 V is applied, the pH value on the anode surface instantaneously falls below 3.8 by electrolysis. However, because during the electrolytic process a pH gradient perpendicular to the electrode grows with the time, different regions of the inverse opal structure feel different pH values, depending on the distance from the electrode. This spatial-temporal change in pH affects the kinetic change in the volume of the porous gel, producing a very slow change of the reflected peak from 800 nm in the initial state to 580 nm in the ionized state.

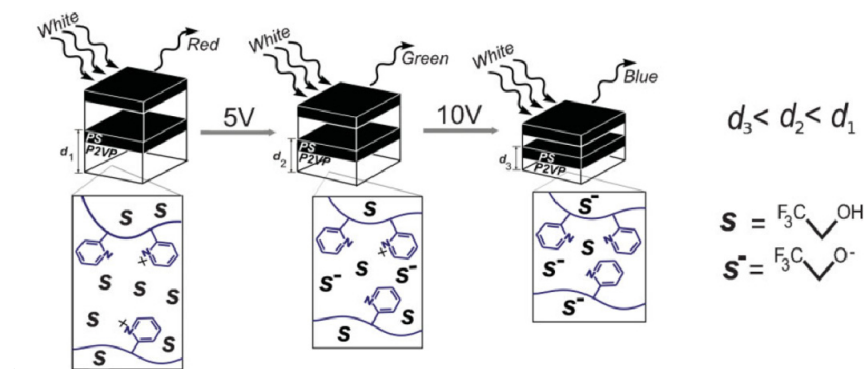


Fig. 6 Schematic representation of the mechanism for electrochemical colour change of PS-P2VP multilayer 1D-PC. Reproduced from ref. 52 with permission of Wiley VCH.

More recently, a bioinspired, electrochemically tunable, full-colour pixel was designed based on a self-assembled block copolymer 1D-PC, that mimics the type of optical response of the reflecting proteins found in certain cephalopod species.⁵² To this purpose, it was exploited the change in pH of a non-aqueous solution caused by an external electric field, resulting in the modification of the thickness and the refractive index of a polyelectrolyte polymer gel. In order to obtain an expansion of the system along a single direction and to magnify the response of the periodic dielectric stack, a multilayer of a diblock copolymer incorporating a glassy domain of polystyrene (PS) and a gel domain of (poly-2-vinylpyridine) (P2VP) was used, together with 2,2,2-trifluoroethanol (TFE) as electrolyte (Fig. 6). At equilibrium there is a finite concentration of H^+ ions in solution due to the autodissociation of TFE into trifluoroethoxide (TFX^-) and H^+ ions. Some of the latter protonate the basic sites of P2VP converting it to a polyelectrolyte (P2VP^+), increasing its solubility in the TFE. When voltage is applied to the cell electrodes and the redox potential is reached, TFE undergoes an electrochemical reaction forming TFX^- at the electrode interface and a pH gradient between the electrodes is formed. Consequently, the degree of ionization of P2VP layers increases, causing an immediate swelling of the polymer and thus a variation of the refractive index. In this way, by applying a voltage of 5 V, it is possible to change the colour from red to

green, or up to blue-green with 10 V.

With the same PS-P2VP copolymer multilayers, system tuning at lower voltages can be achieved using a water/ethanol mixture as the solvent, as reported by Lu *et al.*¹³ In particular, by applying a voltage in the range of 0-2.5 V is sufficient to cause a shift of the diffracted wavelength from blue to red. In this manner, by using a low driving voltage (<2.5 V) it is possible to effectively avoid some side reactions in the solution mixture and to reduce the energy consumption. In addition, a mixture of acetonitrile and water permits to further reduce the driving voltage to 1.2 V to cover the entire visible range. The process is reversible and can be iterated several times, by applying voltages between -2.1 and +2.5 V, although the response times are in the order of several minutes. For instance, it was shown that the reflective peak first shifts from 430 to 640 nm within approximately 15 min and then drastically slows down reaching 660 nm over a long time.

The colour instability of the system and its drifting upon removal of the voltage were resolved by Hwang *et al.*, by using a multilayer of alternating PS and quaternized P2VP domains, modified with phosphate ions and immersed in a salt mixture of methanol and water.¹⁴ This PS-*b*-QP2VP system exhibits a green photonic colour at zero bias voltage, adjustable up to the red region upon application of anodic bias voltage at the working electrode. The band gap can be shifted within few seconds from 526 nm to 610 nm with increasing bias voltage from 0 to 5 V, while the original colour can be restored by applying cathodic bias voltage. Moreover, the red-shifted colour is preserved for several days when the bias is removed.

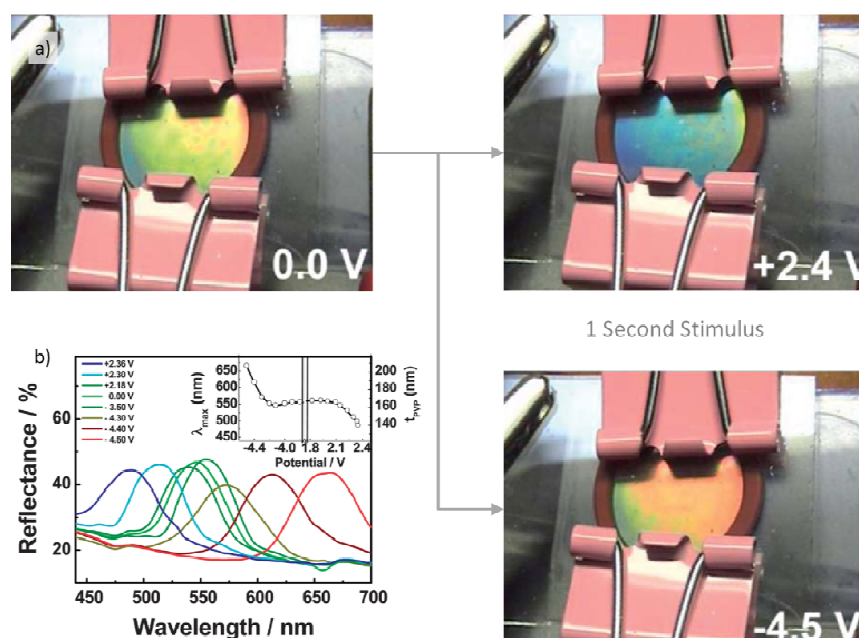


Fig. 7 a) Photographs of colour switching of a quaternized PS-*b*-P2VP thin film at different applied voltage. b) Dependence of reflective spectra of the thin film on the applied electrical potential.

Adapted from ref. 53 with permission of The Royal Society of Chemistry.

Further advances of PS-*b*-QP2VP photonic crystals have been more recently obtained by using a mixture of acetonitrile/water and lithium nitrate as charged ions.⁵³ The reflected peak position can be modulated with the applied voltage, resulting in a full colour display from the ultraviolet to the near-infrared region. In particular, the band gap changes from green to blue when a positive potential is applied and from green to red upon applying a negative potential (Fig. 7). This continuum of the accessible colours is observed over a voltage range of a negative applied potential (-3.5 V – -4.5 V) and positive potential (+2.0 – +2.4 V). When a positive voltage is applied to a quaternized PS-*b*-P2VP photonic crystal, negatively charged nitrate ions bind to the thin film due to Coulomb's attraction, producing a shrinkage of the photonic crystal and then a blue-shift of the reflected peak. On the contrary, when a negative voltage is applied, lithium ions bind to the polymer film so that the local concentration of lithium ions around the film increases. Since P2VP is positively charged, the photonic crystal swells due to the repulsion between the positively charged pyridinium groups and lithium ions, generating a red-shift of the reflective band. One of the most important improvements of this electrically TPC concerns its switching time, which results much shorter than the first reported PS-*b*-P2VP films. In fact, the red and blue shifts are completed within one second revealing the fast migration of the lithium ions through the film.

Another type of electrically TPCs was reported from Wang and Song in the same years, proposing an electrochemical responsive PC based on polypyrrole (PPy), whose electrical properties can be reversibly modulated by doping or dedoping with different ions.⁵⁴ In particular, an inverse opal structure was prepared by electropolymerization of a pyrrole aqueous solution, infiltrated into a colloidal crystal of core-shell nanospheres (hydrophobic polystyrene (PS) core and hydrophilic poly(methyl methacrylate/poly(acrylic acid) (PMMA-PAA) shell). Following the polymerization, the PPy/nanoparticles composite opal was exposed to tetrahydrofuran for 24 h to remove the poly(St-MMA-AA) photonic crystal template. The optical properties of the obtained PPy inverse opal were modulated by redox reactions, carried out in an electrochemical cell filled with aqueous LiClO₄ solution. However, the stop-band position shift was shown to be modest, passing reversibly from about 620 nm at neutral state to about 570 nm at oxidised state. This change of the stop-band was mainly attributed to matrix doping and dedoping of Li⁺, which led to the increase/decrease of both volume and refractive index of PPy.

The same approach of doping/dedoping of polymers was applied by Norton *et al.* with crystal colloidal arrays (see section 4 for a detailed discussion) of PEDOT-coated silica particles, in order to modify the redox state of polymeric shell and, as a consequence, its refractive index.^{55,56} Upon applying negative voltages, a decrease of *ca.* 60 % of the peak was observed, although the reflection wavelength shift was modest (less than 10 nm). This behaviour was attributed to the changes of refractive index of PEDOT layers, accompanied by a slight variation of the interparticle distances.

3 TPCs based on Liquid Crystals (LCs)

3.1 Brief Overview on LC Behaviour under Electric Field

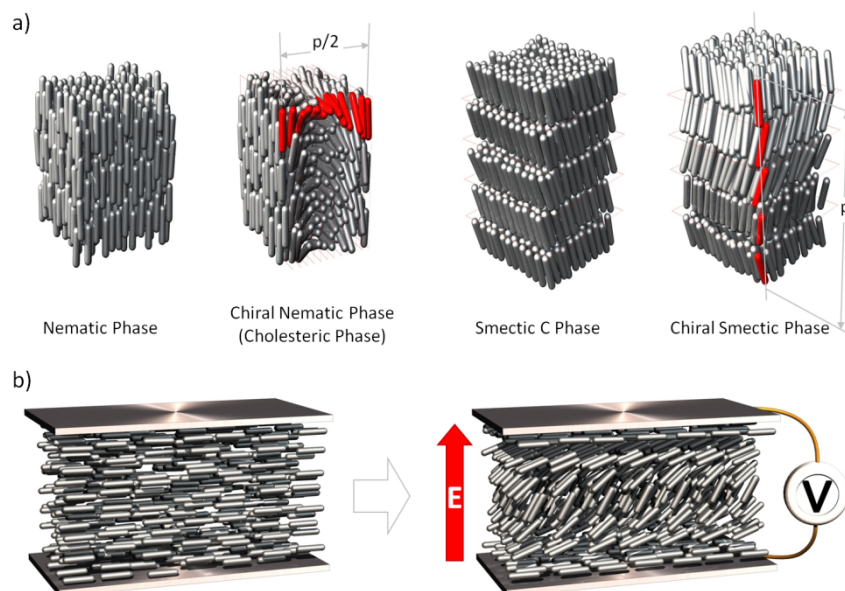


Fig. 8 Schematic representation of (a) molecules arrangement in nematic, chiral nematic, smectic and chiral smectic phase. p is the helix pitch that is the length over which the director rotates 360° . (b) LC alignment changing induced by an external electric field.

5
 Liquid crystals (LCs) are substances in an intermediate state of matter that combines the fluid behaviour, where the molecules are randomly distributed without long-range order, and the properties of solid crystals, in which the atomic or molecular species are packed in highly ordered three-dimensional lattice structures, characterized by a long-range positional and orientational order, as reported in Fig. 8a for rod-shaped molecules. The preferential alignment axis of the molecules is described by a vector, called director. In nematic phase, for example, molecules are randomly distributed as in a liquid, but they self-align maintaining their long axis roughly parallel. In smectic phase, indeed, molecules are organized in distinct layers with a well-defined interlayer spacing. If molecules are organized in a helical arrangement, in which the director orientation gradually rotates along the axis of the helix, chiral liquid crystalline phase results.

LCs are characterized by a strong anisotropy in several physical properties (e.g. elastic, electric, magnetic and optical properties) which depends on the steric factors and polarizability of the molecules contained in these materials.⁵⁸

The most striking anisotropic property is birefringence, which is on the basis of the LC electro-optic properties. As in the case of birefringent crystals, the speed of propagation of light waves in liquid crystalline mediums is no longer uniform but it is dependent upon the direction and the polarization of the incident light. The material possesses different refractive indices in different directions. In particular, the effective refractive index for linear polarized light with the electric field direction along the plane perpendicular to the director (ordinary refractive index n_o or n_\perp) is different from the effective value for polarized light with the electric field direction parallel to the director (extraordinary refractive index n_e or n_\parallel).⁵⁹ The

birefringence, defined as $\Delta n = n_e - n_o = n_{\parallel} - n_{\perp}$, decreases with increasing temperature, due to orientational order loss, and vanishes above the nematic-isotropic transition temperature, above which the molecules are randomly distributed.

5 Similarly to the refractive index, the static dielectric constant ϵ_{\parallel} for an electric field applied parallel to the director, is different from the effective value ϵ_{\perp} observed for a field perpendicular to the director. If the dielectric anisotropy $\Delta\epsilon = \epsilon_{\parallel} - \epsilon_{\perp}$ is positive, the electric polarization for electric field \vec{E} applied parallel to the director is larger than \vec{E} perpendicular to the director. As a consequence, the director tends to
10 align along the field (Fig. 8b). For negative $\Delta\epsilon$, a director orientation in the plane perpendicular to the external field is favourable. The electro-optic switching behaviour of nematic LCs is governed by the competing influences of the director anchoring at interfaces, the alignment of the director field in the bulk due to external fields, and the elastic behaviour of the director field. This competition is referred to
15 as Fredericks transitions⁶⁰ and more detailed and theoretical information on it can be found elsewhere.⁶¹⁻⁶⁵

The possibility to change the orientation of the director and thus the material refractive index by an external voltage can be exploited to obtain electrically tunable PCs. Extensive efforts have been dedicated in recent years in the synthesis of novel
20 mesogens and development of PCs based on LC materials. This is the reason why reporting most of the literature's examples is a quite hard job. As a consequence, in this review only the most significant experiments are analysed in more details and they are classified on the basis of the liquid crystal structure.

3.2 Refractive index modulation

25 PCs containing nematic LCs are fabricated by infiltration of LC molecules into porous regions of the photonic materials, generally opal structures, at a temperature above the nematic-isotropic transition of the LC system, followed by a slow cooling to obtain an ordered nematic phase. The electrical stimulus, i.e. the application of an external electric field across the PC, acts on the molecular director orientation,
30 modifying the refractive index of the filling material. The voltage value needed for LC reorientation obviously depends on the polarizability properties of the molecules used as filling and on the photonic crystal thickness.⁶⁶

For normal incidence geometry, Bragg reflection wavelength λ_{max} is determined by equation 1, which becomes:

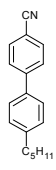
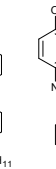
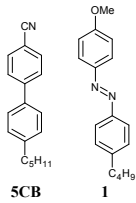
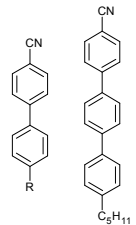
35

$$\lambda_{max} = 2d\sqrt{n_{LC}^2\varphi + n_m^2(1 - \varphi)} \quad (3)$$

where n_{LC} and n_m are respectively the refractive indices of the LC phase and of the other medium. When LCs are infiltrated in opal voids, in absence of an external
40 electric field, n_{LC} can be assumed equivalent to that in the isotropic phase, because of the three-dimensional symmetry of the arrangement and the shape of the voids without an electric field.⁶⁷ As a consequence, the resulting refractive index n_{LC} can be approximated as the mean value n_{ave} between n_o and n_e of the LC. When a bias is applied, LC molecules tend to align along the field direction. If the electric field is
45 parallel to the direction of light propagation, the component of the ordinary refractive index n_o increases and the average refractive index of the LC decreases,

with a consequent shift of the reflected peak toward lower wavelength. The maximum refractive index variation that can be obtained is then $\Delta n = n_{ave} - n_o$. Some notable examples of PCs infiltrated with LCs are summarized in Table 2.

Table 2 Chemical structure of LCs used as filling material of inverted opals. For each compound, several performances of the corresponding TPCs are summarized.

Liquid Crystals	PBG Shift Range	Applied Electric Field	Switching Time	Ref.
 5CB	~ 5 nm	up to 12 V/ μ m	~ 40 μ s	67
 5CB	~ 35 nm	up to 6 V/ μ m	2 ms	68
 5CB 1	~ 20 nm	up to 16 V/ μ m	–	69
 E7 mixture R = -C ₃ H ₁₁ , -C ₇ H ₁₅ , -OC ₈ H ₁₇	10 nm	up to 14 V/ μ m	–	70,71

After the discovery of the techniques to fabricate photonic crystals, the importance and the potentiality to modify refractive indices of the photonic materials with LCs by the applied voltage were very clear, although the first attempts were quite inefficient.^{72–77} At the beginning, in fact, a blue-shift of few nanometers in the reflection spectra of a silica opal infiltrated with 4-pentyl-4'-cyanobiphenyl (5CB) was observed by applying a voltage up to 140 V, corresponding to an electric field of 12 V/ μ m.⁶⁷ Similar results were registered with 4-(*trans*-4-pentylcyclohexyl)-benzonitrile (PCH5) by applying an electric field up to 80 V/ μ m.⁷⁸

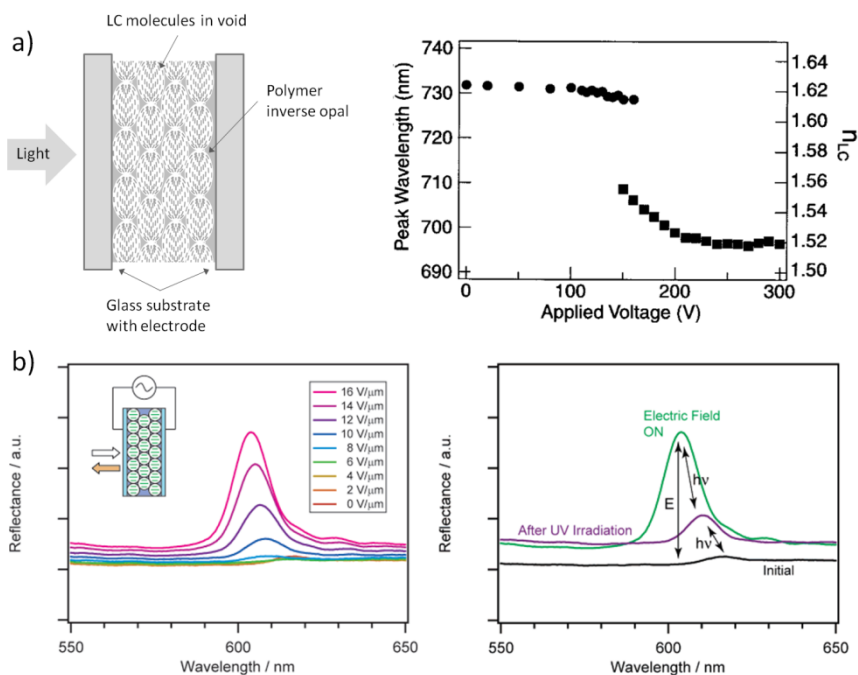


Fig. 9 a) Schematic illustration of polymeric inverse opal film infiltrated with 5CB. The variation of the peak position with the applied voltage is also reported. Adapted from ref. 68 with permission of Wiley VCH. b) Dependence of reflective spectra of the inverse opal film infiltrated with 5CB and **1** mixture (see Table 2) on the applied electric field and its reversible variation upon irradiation with UV or visible light. Reproduced from ref. 69 with permission of the American Chemical Society.

The weak response of opals infiltrated with LCs was attributed to LC confinement in a constricted interstitial geometry, which creates director orientational defects and gives a high surface area to volume ratio of the liquid crystalline phase. Both of these factors contribute to increase the reorientation field and to reduce the LC volume responding at a given voltage. These problems can be minimized by using, instead of an opal structure, an inverse opal, which offers 74 % of empty volume for infiltration of liquid crystals.⁷³

A greater blue-shift of about 35 nm in the reflection spectra was observed using a polymeric inverse opal matrix infiltrated with 5CB as liquid crystal.⁶⁸ In these conditions a voltage dependence of the reflection peak wavelength is evident. In particular, at low voltage only a small peak shift is recorded but at voltage greater than about 150 V (6 V/μm), which represents a clear threshold, a large blue-shift of 35 nm results in very short time (2 ms) (Fig. 9a). However, once a voltage higher than the threshold value is applied and the reflection peak is shifted, recovering of the initial position is not possible even after long time.

Another example of this application was realized more recently by Kubo *et al.*, who reported photo- and electro-tuning of the optical properties of polymeric inverse opal infiltrated with 5CB and 4-Butyl-4'-methoxyazobenzene (**1**) mixture.⁶⁹ After infiltration of LC mixture, the photonic structure showed a low transmittance because of the light scattering in the initial disordered state. Under electric field an increasing of LC reorientation occurs, resulting in an increase of transmittance.

When the electric field becomes sufficiently high ($> 6 \text{ V}/\mu\text{m}$), the molecules are well aligned and the refractive indices become uniform, producing a slight blue-shift of the reflected band of about 20 nm at $16 \text{ V}/\mu\text{m}$. With electric field decreasing, the spectra do not return completely to the initial state and a blue-shifted peak results after the removal of the electric field. After the second cycle, the small change in the peak position can be repeated reversibly and completely. The presence of azobenzene molecules can be exploited to combine the photo-response to the electrical stimulus, to obtain a double control of PC optical properties. In fact, molecules containing azobenzene moieties can undergo to reversible *cis-trans* photo-isomerization, which can destroy the ordered organization of the liquid crystalline phase. By exploiting this behaviour, after the application of the electric field, the optical stop band can be reversibly shifted from 604 to 612 nm by irradiation with UV or visible light, respectively (Fig. 9b).

Tuning of optical properties at lower voltage was obtained more recently by infiltration in a colloidal structure of E7 liquid crystal mixture, composed of 5CB, 7CB, 4-cyano-4-*n*-octyloxy-biphenyl, and 4-cyano-4-*n*-pentyl-*p*-terphenyl.^{70,71} PCs were fabricated by creating an alternating multilayer structure of silicon dioxide and zirconium dioxide nanoparticles, which provided high refractive index contrast. In this way, good band gap efficiency resulted without increasing the crystal thickness that requires high applied electric voltage. In particular, by applying a voltage of only 8 V, corresponding to $3.4 \text{ V}/\mu\text{m}$ as electric field, a blue-shift of 8 nm of the reflected band was observed, although to obtain an additional 2 nm shift a voltage of 32 V was needed.

3.3 Lattice constant modulation

Chiral liquid crystals have a self-organized helical arrangement which can be regarded as a 1D periodic structure and thus a stop band in the transmission spectrum is possible. In these systems, such as Cholesteric Liquid Crystals (CLCs), also called chiral nematic LCs (N*LCs), or chiral smectic LCs, molecules are arranged in a helical structure such that the director orientation change progressively along the axis of the helix (Fig. 8a). These phases show a selective reflection of circularly polarized light if the helical pitch is sufficiently short. In particular, a right-handed structure selectively reflects right circularly polarized light at the Bragg wavelength and is transparent for left circularly polarized light; vice versa for a left-handed structure. The upper (λ_{max}) and lower (λ_{min}) boundaries of the reflected band are $\lambda_{\text{max}} = p n_e$ and $\lambda_{\text{min}} = p n_o$, respectively, where p is the helix pitch, corresponding to the length over which the director rotates 360° . The pitch is determined by the concentration of the chiral components and decreases with an increasing chiral fraction. Tuning of these photonic band gaps is achieved through control of the pitch, which is sensitive to several external stimuli.^{79–81}

The reader interested for more details on tunable photonic liquid crystal could refer to several good reviews^{62,82–87} since this particular topic goes beyond the scope of this review.

4 Colour Tunability by Electrophoretic Forces

At very high concentration, charged monodisperse colloidal systems exhibit photonic stop bands, caused by electrostatic interactions that force particles to organize into ordered structures, called crystalline colloidal arrays (CCA).^{88,89} In

this context, electric field offers a significant opportunity to manipulate the lattice constant of the long-range ordered structure and then its colour, by exploiting the electrophoretic movements of the charged particles towards the oppositely charged electrode. With this approach, kinetic problems related to the solvent or ions diffusion that characterize other techniques for electrical tuning of PCs are avoided, allowing to reach very low switching time with low voltages. In addition, compared with other methods that require polymer synthesis and all the procedures related to the inverse opals fabrications, this methodology results more convenient and less time-consuming.

In this type of dynamic photonic structures, assuming that the colloids form face-centered cubic (fcc) structures with (111) planes parallel to each of two electrodes, the reflection wavelength for normal incident light can be estimated by a modification of equation 1:⁹⁰

$$\lambda = \left(\frac{\pi}{3\sqrt{2}\varphi} \right)^{\frac{1}{3}} \left(\frac{8}{3} \right)^{\frac{1}{2}} D \sqrt{n_p^2 \varphi + n_m^2 (1 - \varphi)}$$

where D is the particle diameter, n_p and n_m are the refractive indices of the particles and medium, respectively, and φ is the volume fraction of the charged particles near the oppositely charged electrodes.

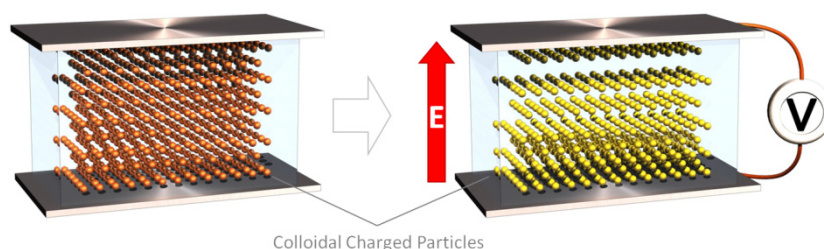
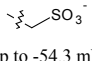
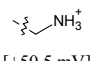
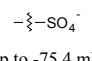
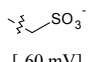
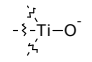


Fig. 10 Schematic representation of electrophoretic compression of crystalline colloidal arrays (CCA) towards the oppositely charged electrode. The change of the interparticle distances determines a shift of the reflected wavelengths.

Upon applying voltage, the particles move towards the oppositely charged electrode by coulombic forces (Fig. 10). Due to their high charge and in order to minimize the total repulsive energy, particles tend to arrange into ordered structures, leading to a variation of φ and, as a consequence, of λ . However, the understanding of the effective mechanism related to the changes of inter-particle distance is quite difficult. Indeed, even in the case of non-interacting particles, under the application of an electric field, in addition to the electrophoretic force, there are numerous complex forces, such as frictional, retardation, and relaxation forces.^{91,92} Several examples of electrophoretically tunable colloidal crystals are summarized in Table 3.

Table 3 Surface charged groups of nanoparticles used to construct crystalline colloidal arrays. For each system several performances are summarized.

Nanoparticles	Superficial Charged Groups ^a	PBG Shift Range	Applied Electric Field	Switching Time ^b	Ref.
PS	 [up to -54.3 mV]	~ 505 – 605 nm	up to ~ 0.035 V/μm	< 1 s	90
	 [+50.5 mV]	similar range	up to ~ 0.035 V/μm	< 1 s	
PMMA-PS	 [up to -75.4 mV]	450 – 650 nm	up to 0.035 V/μm	> 1 min	93
ZnS@SiO ₂	 [-60 mV]	450 – 650 nm	up to 0.032 V/μm	–	94
SiO ₂ @TiO ₂	 [-37.4 mV]	Visible range ^c	up to 0.025 V/μm	–	95

^a In square brackets are reported the measured Zeta potentials.

^b Not reported if they are not specified.

^c The reflection spectra are quite complex.

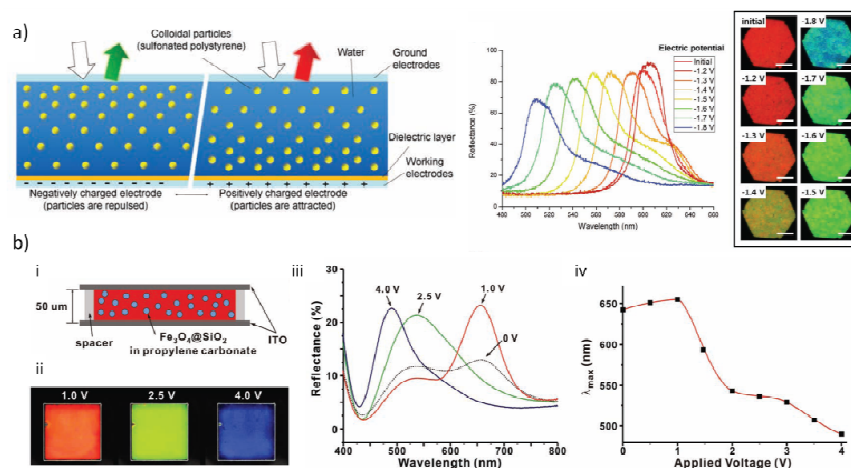


Fig. 11 a) Schematic representation of electrophoretic compression of sulfonated PS-NPs colloidal arrays and its electrical potential dependence of reflective spectra. Photographs of colour tuning at different voltages are also reported. Reproduced from ref. 90 with permission of Wiley VCH. b) i.

10 Schematic structure of photonic display pixel based on colloidal dispersion of Fe₃O₄@SiO₂ nanoparticles. ii. Photographs of colour tuning at different voltages. iii. Dependence of reflective spectra of the photonic display pixel on the applied electrical potential. iv. Variation of the peak position with the applied voltage. Adapted from ref. 96 with permission of Wiley VCH.

Although this approach was proposed several years ago,^{97–99} a real example of electrical modulation of a colloidal lattice of highly charged particles was more recently obtained by infiltrating between two ITO glass slides a highly sulfonated PS suspension.⁹⁰ When a voltage is applied, the electrokinetic forces acting on the PS nanoparticles determine the compression of the colloidal lattice as long as it is not balanced from the electrostatic repulsive forces among the particles. Therefore, with moving away from the attracting electrode, each layer of particles is stopped by the repulsive forces exerted by the layers closer to the electrode. As a consequence, the magnitude of compression and of the band gap shift can be controlled by varying the electric field intensity. In particular, as the authors demonstrated, when the charge on the working electrode periodically varies in case of AC field, the colloidal arrays experience repeated compressions and relaxations. This effect induces a periodic modulation of the reflection colour that, in turn, results in an alternating blue and red-shifting of the band gap. The extent of the shift increases with increasing the electric field and the colour variations are reversible and stable over more than 12 000 cycles (~ 40 min) with no appreciable deviation in terms of shift and intensity. Under a DC field applied between 0 V and -1.8 V, the reflectance band can be rapidly shifted up to 100 nm, covering from red to blue colours in the optical images (Fig. 11a).

By using concentrated suspensions of copolymer poly(methyl methacrylate)-polystyrene (PMMA-PS) particles, Han *et al.* obtained crystalline colloidal arrays that were tunable on a wide range of wavelength with low voltage.⁹³ In particular, the resulting structural colour, which depend on the PS and PMMA ratio and on the particle diameter and suspension concentration, can be modulated from red to blue by applying a voltage lower than 3.5 V (electric field up to 0.035 V/ μm).

To improve the optical properties of the photonic structure, high refractive index materials can be used. Based on this idea, an highly sulfonated silica-coated ZnS nanoparticles dispersion was employed, allowing to obtain a very active full colour display.⁹⁴ In fact, in the static state, the photonic structural colours are very strong, with a reflectance around 90 % in red, green and blue regions depending on the particle concentration of the used suspension. Under the application of electric field, particles move towards the positive electrode, producing an increase of the average population of particles near this electrode. As a consequence, because the general order of the particles is maintained due to their strong electrostatic repulsion, a shift of the PBG toward shorter wavelength is observed. In particular, a shift of the reflected peak position from red (650 nm) to blue (450 nm) is achieved upon applying a voltage in the range from 0 to 3.2 V, allowing a full colour manipulation. However, with the increase of the applied voltage, the reflectance falls below 30 %.

A similar example, based on the use of TiO₂-coated silica nanoparticles suspension, was reported by Luo *et al.*, although in this case low control of the reflection bands for several shell thickness was observed.⁹⁵

A version with positively charged nanoparticles was even proposed, by functionalization of TiO₂ nanoparticles with (3-trimethoxysilylpropyl) diethylenetriamine. However, upon applying electric field only a low variation of the intensity of the reflected wavelength band is observed.¹⁰⁰

A common disadvantage of these examples concerns the absence of a complete PBG that implies a strong angle dependence of the reflected wavelength, thus limiting their implementation in real technological application. However, this

problem can be overcome by applying quasi-amorphous materials, which are colloidal structures with only short-range order on length scales comparable to optical wavelengths but without lattice periodicity or long-range order.^{89,101} While crystallization is preferential for typical monodisperse colloidal particles, random arrangement are favourite when the polydispersity of particles is moderately high ($\delta > 7\%$) and/or the particle concentration is above a critical concentration.^{102,103} In addition to hold a PBG, quasi-amorphous structures show characteristic angle-independent and non-brilliant photonic colours due to the coherent scattering of light from the isotropic nanostructures with short-range order. The reflected wavelength is determined by the average inter-particle distance, which can be manipulated to obtain a tunable photonic material.

By applying this idea, Lee *et al.* demonstrated the fabrication of electrically tunable full-colour photonic pixel, based on silica-coated Fe_3O_4 nanoparticles with high polydispersity index.⁹⁶ The system is able to change its colour from red to blue by applying a voltage up to 4 V (electric field up to $0.08 \text{ V}/\mu\text{m}$) (Fig. 11b). As expected from amorphous structures, an overall angle independency is observed. In fact, the reflected wavelength peak at 40° incidence shifts of only 5 nm with respect to the normal reflected peak. In addition, very short response times are recorded, allowing on-switching (from 0 V to 4V) and off-switching (from 4 V to 0 V) in 50 ms and 170 ms respectively.

The electrophoretically induced compression of the photonic structure can be applied not only on colloidal crystals but also on inverse opals that are constituted by charged polymeric matrices. In particular, the polyelectrolyte gel of poly(HEMA-co-MAPTA- PF_6), obtained from the free-radical polymerization of 2-hydroxyethyl metacrylate (HEMA) and [3-(methacryloylamino)propyl]trimethylammonium hexafluorophosphate (MAPTA- PF_6), contains chains with immobilized positive charges, which can easily dissociate from their counter anions PF_6^- even in organic solvents because of their weak ionic interaction.¹⁰⁴

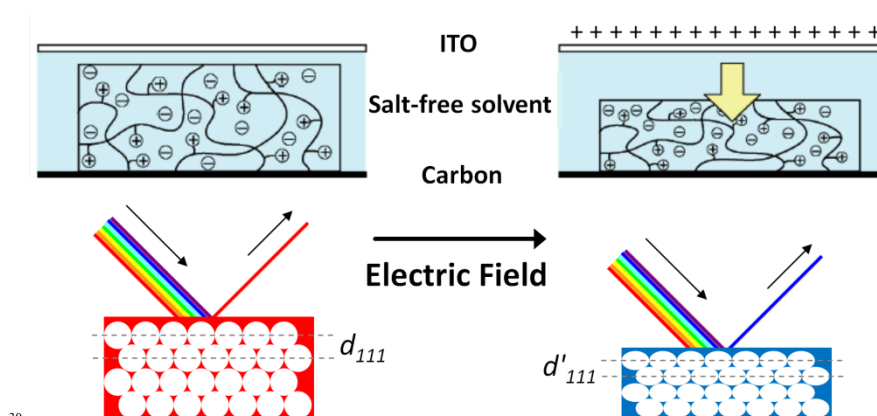


Fig. 12 Schematic representation of colour change mechanism of polyelectrolyte gel inverse opal upon the application of an electric field. Adapted from ref. 104 with permission of The Royal Society of Chemistry.

A thin inverse opal film, prepared with this polymeric hydrogel, is placed between

an ITO glass slide and a carbon electrode and then filled with a salt-free organic solvent mixture of dimethylformamide and 1,4-dioxane. After the application of an electric field a contraction of the lattice spacing is observed. This behaviour can be explained with the electrophoretic forces that drag the cations toward the cathode and their dissociated counter anions toward the anode (Fig. 12). In this way, it is possible to change the inverse opal colour from green to blue with voltages of 10-30 V (electric field up to 0.015 V/ μm), even if a shift of 60 nm upon applying 12 V is completed after about 60 s.

In this type of devices based on electrophoretic forces, the use of aqueous colloidal dispersion permits to reduce the energy barrier that must be surmounted to charge separation because of the higher dielectric constant of water with respect to most organic solvents. However, one problem related to use water as the solvent concerns the poor tuning repeatability originated from unwanted ion generation at the electrode surface and its diffusion into the colloidal dispersion when the applied potential is above the minimum potential required for reduction and oxidation.¹⁰⁵

With increasing of repeated cycles, this phenomena cause a decrease of repulsive forces among particles, which result in shorter equilibrium distance, and at certain voltages the PBG position does not remain constant. In order to prevent or at least to minimize the diffusion of ions, some efforts were made,^{105,106} although a better control of the PBG is needed.

5 Indirect Electrical Tuning of PCs

In all of the examples seen until now, the applied electric field represents an external stimulus that directly modifies some material properties, in order to obtain a colour change of the photonic system. In the case of electrochemical processes, for instance, the electric field induces a change of the redox state of some groups inside the polymeric structures which play a leading role in the PCs colour changes. Similarly, in the case of LCs, electric field directly modifies the refractive index of the filling material, inducing a shift of the PBG.

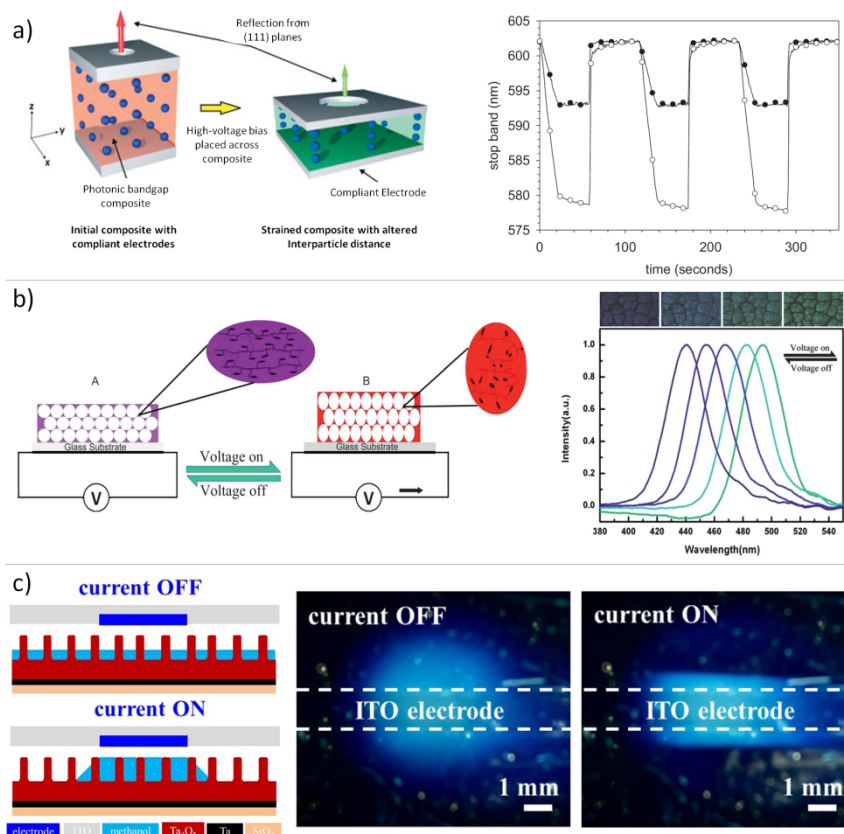


Fig. 13 a) Schematic representation of the mechanism for electric field induced colour tuning by compression of a dielectric elastomeric PC. When a voltage is applied on the electrodes a contraction along the z axis is obtained, which results in a modification of the interparticle distances and then in a blue-shift of the reflected light. The variation of the reflected wavelength with the applied electric field ($12.5 \text{ V}/\mu\text{m}$ (\bullet) and $25 \text{ V}/\mu\text{m}$ (\circ)) is also reported. Reproduced from ref. 107 with permission of Wiley VCH. b) Schematic illustration of the mechanism for the colour change of inverse opal film based on thermoresponsive liquid crystal elastomers and its voltage dependence of reflective spectra of the photonic structure. Reproduced from ref. 108 with permission of The Royal Society of Chemistry. c) Schematic representation of the mechanism for the variation of solvent distribution inside the nanoglass when current is applied to the ITO electrode. Photographs of electrically-induced colour switching of Ta_2O_5 nanoglass infiltrated with methanol are reported. Reproduced from ref. 109 with permission from OSA's Optics InfoBase.

However, in contrast to these examples, electric field can be exploited as secondary stimulus, able to induce a process that acts as primary stimulus for the desired property variation. Electric field, therefore, determines only indirectly a colour change in the case of TPCs but the same result could be obtained with other stimulation. This type of approach is widely used, for instance, in dielectric elastomer actuators and artificial muscles field,¹¹⁰ exploiting the squeezing process of a dielectric material sandwiched between two charged electrodes (Maxwell stress).¹¹¹ The same outcome could be obtained by applying a suitable external pressure. From a practical point of view, the electrostriction can be very fast although a voltage of several kV is needed, to obtain the electrostatic attraction of

two electrodes separated by a dielectric material layer with suitable thickness.

Based on this technology, Xia *et al.* proposed an electric-field induced tuning of the PBG by straining of a polymeric opal with two silicone-carbon black composite electrodes.¹⁰⁷ When voltage is applied, the opal film is compressed, resulting in a variation of interparticle distances and then in a blue-shift of the reflected light (Fig. 13a). In addition, by applying an electric field of 25 V/ μm a shift of 25 nm of the stop band is observed and the colour tuning can be repeated several times with high reproducibility, although the switching process requires more than a few seconds.

Similar approach was reported later by Fang *et al.*, who recorded a reflected peak shift of 30 nm by applying a voltage of 3 kV (100 V/ μm) on an opal of PS nanoparticles infiltrated with poly(dimethyl siloxane) (PDMS).¹¹² Another example was reported by using water as compliant and transparent electrodes, which allowed a very fast and reversible blue-shift of polymeric opal PBG up to 60 nm with electric field up to 20 V/ μm .¹¹³

Infiltration of LC in photonic structures allows the electrical tuning of the PBG, even though the obtainable changes in the optical properties are quite limited, because of the limited free volume inside the crystals. This limitation was surpassed by Jiang *et al.* through fabrication of an electrothermally active inverse opal, based on a thermoresponsive liquid crystal elastomer.¹⁰⁸ The response of this material, in terms of matrix expansion/contraction, depends on the temperature which can be modulated via Joule heating by driving an electric current through a conductive graphite layer embedded into the glass support (Fig. 13b). In this type of device, therefore, the applied voltage is a secondary stimulus that serves to produce heat and increase the temperature, which represents the primary stimulus. In fact, a similar effect could be performed by external heating of the polymeric matrix. The elastomeric matrices were prepared by photo-polymerization of infiltrated 4-(6-acryloxyhexyloxy)-4'-cyanobiphenyl, used as mesogenic moiety, and different quantity of 1,6-hexanediol diacrylate as cross-linker. With increasing the voltage and then the temperature, the aligned liquid crystal moieties become isotropic and an expansion of the inverse opal structure takes place. As a result, the reflection peaks shift drastically toward longer wavelength with continuous changing of structural colour. The degree and the reversibility of the electrothermal response depend on the cross-linking density. Under optimized conditions, shifts of 60-80 nm can be obtained by applying a voltage of 30 V, although several seconds are needed for the switching processes.

The resistive heating that results by applying a voltage on conductive glass slides was recently exploited to induce a variation of surface tension of solvents infiltrated into a tantalum pentoxide (Ta_2O_5) nanograss.¹⁰⁹ In particular in absence of voltage, the solvent inside the nanostructured layer is uniformly distributed, generating a uniform blue coloration (Fig. 13c). Upon applying voltages to the ITO electrode placed on top of the nanograss surface, colour switching in the area not covered by the electrode occurs. This behaviour can be explained by thermal variation of surface tension that drives the solvent under the ITO electrode.

6 Conclusions and Outlook

Tunable PCs constitute an important class of intelligent systems that are able to convert an external stimulus into an optical response. Among these, electrical stimulus represents the most promising approach to control in easy and convenient

way the photonic properties and permits to foresee an implementation in real technologies, such as displays, sensors and other colour material applications. Based on these potentialities, in the last fifteen years the research in this area has mainly focused on finding methods to electrically tune the PBG position with low voltages and low switching time.

Each strategy offers some advantages but, considering real technological applications, additional improvements are needed. For example, a common disadvantage regards the side reactions of oxidation and reduction of solvent at the electrodes: beside increasing the energy consumption, such reactions generate gaseous species, which have to be removed from the cell. This challenge can be surpassed by using non-aqueous solvents and, as in the case of electrochemically TPCs, more expensive electrolytes. Otherwise, especially in the cases where the current flow is not necessary, it would be possible to cover the electrodes surface with a thin transparent insulator layer, although an increasing of the voltage is needed. Another general aspect to keep into account concerns the use of liquid solutions, which could make difficult the implementation of this technology in patterned or flexible substrates.

Considering the electrochemical processes, for example, in which reduction and oxidation reactions modify the refractive index and the lattice constant of the photonic structure, the PBG tuning can be realized on a wide wavelength range with low voltages, even if the switching time are often limited by diffusion kinetics of ions and solvent molecules. In addition, the production of these systems is in general more expensive and time consuming, if we consider the several steps (NPs synthesis and deposition, polymeric inverse opal fabrication and electrochemical cell assembling) that have to be performed before to reach a functioning 3D tunable PC.

On the contrary, PCs based on LCs allow to avoid the use of liquid solution and the problems connected with it. Moreover, they show very fast responses, even though the changing colour ranges are unfortunately quite restricted.

Regarding the electrophoretically tunable crystalline colloidal arrays, despite further studies and optimizations are however necessary to reach high cycle rates without loss of control of the PBG position, these systems are more easily processable and promising. In fact, they do not need long processes of fabrication, as well as the use of dangerous substances for template etching (e.g. hydrofluoric acid). These devices can be easily assembled allowing fast colour tuning on a wide range with low voltages.

A summary of the several advantages/disadvantages for each type of electrically TPCs is reported in Table 4, together with a brief outlook on possible improvements. The TPC based on indirect electrical methods are not included in this Table because of the lower performances with respect to the other approaches.

Table 4 General comparison between the several working principles applied for the fabrication of electrically TPCs.

Working Principle	Advantages	Disadvantages	Possible Improvements
Electrochemical Processes	<ul style="list-style-type: none"> Wide PBG shift range Low voltages Reversibility 	<ul style="list-style-type: none"> High switching times Use of solvents Use of electrolytes Possible hysteresis Long fabrication procedures 	<ul style="list-style-type: none"> Reducing the switching time Using of economic polymers Increasing of the reflectivity efficiency
Reorientation of LCs	<ul style="list-style-type: none"> Very fast switching Low voltages Reversibility Ease fabrication Absence of solvents 	<ul style="list-style-type: none"> Very small PBG shift range High cost of LCs 	<ul style="list-style-type: none"> Increasing of the PBG shift range
Electrophoretic Assembling of Colloids	<ul style="list-style-type: none"> Wide PBG shift range Low voltages Low switching times Possible angle-independent colour Reversibility Ease fabrication 	<ul style="list-style-type: none"> Use of solvents Possible hysteresis 	<ul style="list-style-type: none"> Decreasing hysteresis Reducing switching time

Additional efforts are needed to improve these technologies in view of real technological applications, especially to obtain high durability, angle-independent colours, fast switching and high reflection efficiency. Opportunities for further improvements exist through both optimization of existing materials and design of novel, complex structures.

References

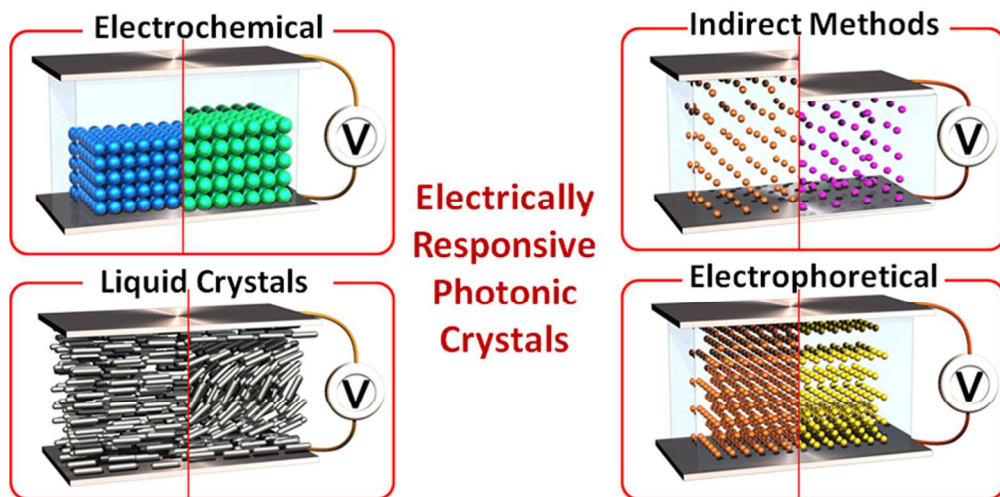
- ¹⁰ ^a The BioRobotics Institute, Scuola Superiore Sant'Anna, Viale Rinaldo Piaggio 34, 56025 Pontedera (PI), Italy.
- ^b Center for Micro-BioRobotics @SSSA, Istituto Italiano di Tecnologia, Viale Rinaldo Piaggio 34, 56025 Pontedera (PI), Italy.
- E-mail: luca.nucara@sss.it, francesco.greco@iit.it, virgilio.mattoli@iit.it.
- ¹⁵
- J. Joannopoulos, S. Johnson, J. Winn and R. Meade, *Photonic crystals: molding the flow of light*, Princeton University Press, New Jersey, USA, 2nd ed., 2008.
 - K. Yu, T. Fan, S. Lou and D. Zhang, *Prog. Mater. Sci.*, 2013, **58**, 825–873.
 - J. Sun, B. Bhushan and J. Tong, *RSC Adv.*, 2013, **3**, 14862.
 - ²⁰ Y. Takeoka, *J. Mater. Chem. C*, 2013, **1**, 6059.
 - C. López, *Adv. Mater.*, 2003, **15**, 1679–1704.
 - J. Joannopoulos, P. Villeneuve and S. Fan, *Nature*, 1997, **386**, 143–149.
 - C. López, *J. Opt. A Pure Appl. Opt.*, 2006, **8**, R1–R14.
 - C. M. Soukoulis, *Photonic Band Gap Materials*, Kluwer Academic Publishers, 1996.
 - ²⁵ S. Sun, C. B. Murray, D. Weller, L. Folks and A. Moser, *Science*, 2000, **287**, 1989–1992.

- 10 B. J. Siwick, O. Kalinina, E. Kumacheva, R. J. D. Miller and J. Noolandi, *J. Appl. Phys.*, 2001, **90**, 5328–5334.
- 11 B. H. H. Pham, I. Gourevich, J. K. Oh, J. E. N. Jonkman and E. Kumacheva, *Adv. Mater.*, 2004, **16**, 516–520.
- 5 12 A. C. Arsenault, D. P. Puzzo, I. Manners and G. a. Ozin, *Nat. Photonics*, 2007, **1**, 468–472.
- 13 Y. Lu, H. Xia, G. Zhang and C. Wu, *J. Mater. Chem.*, 2009, **19**, 5952–5955.
- 14 K. Hwang, D. Kwak, C. Kang, D. Kim, Y. Ahn and Y. Kang, *Angew. Chemie Int. Ed.*, 2011, **50**, 6311–4.
- 15 Y.-J. Lee and P. V. Braun, *Adv. Mater.*, 2003, **15**, 563–566.
- 16 W. Hong, X. Hu, B. Zhao, F. Zhang and D. Zhang, *Adv. Mater.*, 2010, **22**, 5043–7.
- 17 H. Xu, P. Wu, C. Zhu, A. Elbaz and Z. Z. Gu, *J. Mater. Chem. C*, 2013, **1**, 6087.
- 18 H. Fudouzi and Y. Xia, *Adv. Mater.*, 2003, **15**, 892–896.
- 19 J. Ge, J. Goebel, L. He, Z. Lu and Y. Yin, *Adv. Mater.*, 2009, **21**, 4259–4264.
- 20 R. W. Ryan, T. Wolf, R. F. Spetzler, S. W. Coons, Y. Fink and M. C. Preul, *J. Neurosurg.*, 2010, **112**, 434–443.
- 21 E. Yablonovitch, *Phys. Rev. Lett.*, 1987, **58**, 2059–2062.
- 22 J. F. Galisteo-López, M. Ibisate, R. Sapienza, L. S. Froufe-Pérez, A. Blanco and C. López, *Adv. Mater.*, 2011, **23**, 30–69.
- 23 J. Ge and Y. Yin, *Angew. Chemie Int. Ed.*, 2011, **50**, 1492–522.
- 24 J. Y. Wang, Y. Cao, Y. Feng, F. Yin and J. P. Gao, *Adv. Mater.*, 2007, **19**, 3865–3871.
- 25 Y. Kang, J. J. Walish, T. Gorishnyy and E. L. Thomas, *Nat. Mater.*, 2007, **6**, 957–960.
- 26 T. Kanai, D. Lee, H. C. Shum, R. K. Shah and D. a Weitz, *Adv. Mater.*, 2010, **22**, 4998–5002.
- 27 H. Sugiyama, T. Sawada, H. Yano and T. Kanai, *J. Mater. Chem. C*, 2013, **1**, 6103.
- 28 M. Chen, L. Zhou, Y. Guan and Y. Zhang, *Angew. Chemie Int. Ed.*, 2013, **52**, 9961–5.
- 29 X. Xu, G. Friedmann and K. Humfeld, *Chem. Mater.*, 2002, **14**, 1249–1256.
- 30 L. He, Y. Hu, H. Kim, J. Ge, S. Kwon and Y. Yin, *Nano Lett.*, 2010, **10**, 4708–4714.
- 31 L. He, M. Wang, J. Ge and Y. Yin, *Acc. Chem. Res.*, 2012, **45**, 1431–40.
- 32 H. Fudouzi and T. Sawada, *Langmuir*, 2006, **22**, 1365–8.
- 33 E. P. Chan, J. J. Walish, E. L. Thomas and C. M. Stafford, *Adv. Mater.*, 2011, **23**, 4702–6.
- 34 Z.-Z. Gu, T. Iyoda, a. Fujishima and O. Sato, *Adv. Mater.*, 2001, **13**, 1295.
- 35 M. Kamenjicki, I. K. Lednev, a. Mikhonin, R. Kesavamoorthy and S. a. Asher, *Adv. Funct. Mater.*, 2003, **13**, 774–780.
- 36 Z.-Y. Xie, L.-G. Sun, G.-Z. Han and Z.-Z. Gu, *Adv. Mater.*, 2008, **20**, 3601–3604.
- 37 Z. Q. Sun, X. Chen, J. H. Zhang, Z. M. Chen, K. Zhang, X. Yan, Y. F. Wang, W. Z. Yu and B. Yang, *Langmuir*, 2005, **21**, 8987–91.
- 38 Y. Hu, J. Wang, H. Wang, Q. Wang, J. Zhu and Y. Yang, *Langmuir*, 2012, **28**, 17186–17192.
- 39 X. Ye, Y. Li, J. Dong, J. Xiao, Y. Ma and L. Qi, *J. Mater. Chem. C*, 2013, **1**, 6112–6119.
- 40 I. D. Hosein and C. M. Liddell, *Langmuir*, 2007, **23**, 10479–85.
- 41 A. Stein, B. E. Wilson and S. G. Rudisill, *Chem. Soc. Rev.*, 2013, **42**, 2763–2803.
- 42 C. I. Aguirre, E. Reguera and A. Stein, *Adv. Funct. Mater.*, 2010, **20**, 2565–2578.
- 43 Z. Wang, J. Zhang, J. Xie, C. Li, Y. Li, S. Liang, Z. Tian, T. Wang, H. Zhang, H. Li, W. Xu and B. Yang, *Adv. Funct. Mater.*, 2010, **20**, 3784–3790.
- 44 Z. Wang, J. Zhang, J. Xie, Z. Wang, Y. Yin, J. Li, Y. Li, S. Liang, L. Zhang, L. Cui, H. Zhang and B. Yang, *J. Mater. Chem.*, 2012, **22**, 7887.
- 45 J. J. Walish, Y. Fan, A. Centrone and E. L. Thomas, *Macromol. Rapid Commun.*, 2012, **33**, 1504–9.
- 46 J. Hung, M. H. Kok and W. Y. Tam, *Appl. Phys. Lett.*, 2009, **94**, 014102.
- 47 E. P. Chan, J. J. Walish, A. M. Urbas and E. L. Thomas, *Adv. Mater.*, 2013, **25**, 3934–47.
- 48 Y. Zhao, Y. Ying and Q. Wang, *Opt. Laser Technol.*, 2014, **64**, 278–287.
- 49 X. Sui, X. Feng, M. a. Hempenius and G. J. Vancso, *J. Mater. Chem. B*, 2013, **1**, 1658.
- 50 D. P. Puzzo, A. C. Arsenault, I. Manners and G. a Ozin, *Angew. Chemie Int. Ed.*, 2009, **48**, 943–7.
- 51 K. Ueno, K. Matsubara, M. Watanabe and Y. Takeoka, *Adv. Mater.*, 2007, **19**, 2807–2812.
- 52 J. J. Walish, Y. Kang, R. a. Mickiewicz and E. L. Thomas, *Adv. Mater.*, 2009, **21**, 3078–3081.
- 53 Y. Lu, C. Meng, H. Xia, G. Zhang and C. Wu, *J. Mater. Chem. C*, 2013, **1**, 6107–6111.
- 54 L. Xu, J. Wang, Y. Song and L. Jiang, *Chem. Mater.*, 2008, **20**, 3554–3556.
- 55 J. Norton, M. G. Han, P. Jiang, S. Creager and S. H. Foulger, *J. Mater. Chem.*, 2007, **17**, 1149.
- 56 J. C. S. Norton, M. G. Han, S. Creager and S. H. Foulger, *Int. J. Electrochem. Sci.*, 2012, **7**, 3627–3637.

- 57 A. C. Arsenault, H. Míguez, V. Kitaev, G. a. Ozin and I. Manners, *Adv. Mater.*, 2003, **15**, 503–507.
- 58 M. Warner and E. M. Terentjev, *Liquid Crystal Elastomers*, Oxford University Press, 2009.
- 59 K. Busch, S. Lolkes, R. B. Wehrspohn and H. Foll, *Photonic Crystals: Advances in Design, Fabrication, and Characterization*, Wiley-VCH Verlag, Germany, 2004.
- 60 P. G. de Gennes and J. Prost, *The Physics of Liquid Crystals*, Oxford University Press, Oxford, 1994.
- 61 D. A. Dunmur and P. Palffy-Muhoray, *J. Phys. Chem.*, 1988, **92**, 1406–1419.
- 62 S. P. Palto, L. M. Blinov, M. I. Barnik, V. V. Lazarev, B. A. Umanskii and N. M. Shtykov, *Crystallogr. Reports*, 2011, **56**, 622–649.
- 63 V. Tkachenko, a a Dyomin, G. V Tkachenko, G. Abbate and I. a Sukhoivanov, *J. Opt. A Pure Appl. Opt.*, 2008, **10**, 055301.
- 64 J. A. Reyes, J. a. Reyes-Avendaño and P. Halevi, *Opt. Commun.*, 2008, **281**, 2535–2547.
- 65 H. Takeda and K. Yoshino, *Phys. Rev. E*, 2003, **67**, 056607.
- 66 L. M. Blinov, *Structure and the Properties of Liquid Crystals*, Springer, 2011.
- 67 Y. Shimoda, M. Ozaki and K. Yoshino, *Appl. Phys. Lett.*, 2001, **79**, 3627.
- 68 M. Ozaki, Y. Shimoda, M. Kasano and K. Yoshino, *Adv. Mater.*, 2002, **14**, 514–518.
- 69 S. Kubo, Z.-Z. Gu, K. Takahashi, A. Fujishima, H. Segawa and O. Sato, *Chem. Mater.*, 2005, **17**, 2298–2309.
- 70 L. Criante and F. Scotognella, *Mol. Cryst. Liq. Cryst.*, 2013, **572**, 31–39.
- 71 L. Criante and F. Scotognella, *J. Phys. Chem. C*, 2012, **116**, 21572–21576.
- 72 K. Y. Yoshino, S. Satoh, Y. Shimoda, Y. Kawagishi, K. Nakayama and M. Ozaki, *Jpn. J. Appl. Phys.*, 1999, **38**, L961–L963.
- 73 K. Busch and S. John, *Phys. Rev. Lett.*, 1999, **83**, 967–970.
- 74 S. John and K. Busch, *J. Light. Technol.*, 1999, **17**, 1931–1943.
- 75 S. Leonard, J. Mondia, H. Van Driel, O. Toader, S. John, K. Busch, A. Birner, U. Gosele and V. Lehmann, *Phys. Rev. B*, 2000, **61**, 2389–2392.
- 76 Q.-B. Meng, C.-H. Fu, S. Hayami, Z.-Z. Gu, O. Sato and a. Fujishima, *J. Appl. Phys.*, 2001, **89**, 5794.
- 77 P. Mach, P. Wiltzius, M. Megens, D. Weitz, K. Lin, T. Lubensky and a. Yodh, *Phys. Rev. E*, 2002, **65**, 031720.
- 78 D. Kang, J. MacLennan, N. Clark, A. Zakhidov and R. Baughman, *Phys. Rev. Lett.*, 2001, **86**, 4052–4055.
- 79 H. Finkelmann, S. T. Kim, A. Muñoz, P. Palffy-Muhoray and B. Taheri, *Adv. Mater.*, 2001, **13**, 1069–1072.
- 80 Y. Huang, Y. Zhou, C. Doyle and S.-T. Wu, *Opt. Express*, 2006, **14**, 1236–1242.
- 81 Y. Hirota, Y. Ji, F. Serra, A. R. Tajbakhsh and E. M. Terentjev, *Opt. Express*, 2008, **16**, 5320–5331.
- 82 J. Beeckman, *Opt. Eng.*, 2011, **50**, 081202.
- 83 R. Asquini and A. D'Alessandro, in *Proc. SPIE 8828, Liquid Crystals XVII, 88280T (September 12, 2013)*, 2013, vol. 8828, p. 88280T–14.
- 84 S. Furumi, *Polym. J.*, 2012, **45**, 579–593.
- 85 V. I. Kopp, Z.-Q. Zhang and A. Z. Genack, *Prog. Quantum Electron.*, 2003, **27**, 369–416.
- 86 L. De Sio, N. Tabiryan, T. Bunning, B. R. Kimball and C. Umeton, in *Progress in Optics*, Elsevier, 2013, vol. Volume 58, pp. 1–64.
- 87 M. Ozaki, Y. Matsuhisa, H. Yoshida, R. Ozaki and a. Fujii, *Phys. Status Solidi*, 2007, **204**, 3777–3789.
- 88 S. Asher, J. Holtz, L. Liu and Z. Wu, *J. Am. Chem. Soc.*, 1994, **43**, 4997–4998.
- 89 K. Ueno, A. Inaba, Y. Sano, M. Kondoh and M. Watanabe, *Chem. Commun.*, 2009, 3603–5.
- 90 T. S. Shim, S.-H. Kim, J. Y. Sim, J.-M. Lim and S.-M. Yang, *Adv. Mater.*, 2010, **22**, 4494–8.
- 91 M. Evers, N. Garbow, D. Hessinger and T. Palberg, *Phys. Rev. E*, 1998, **57**, 6774–6784.
- 92 J. a Ferrar and M. J. Solomon, *Soft Matter*, 2015, **11**, 3599–3611.
- 93 M. G. Han, C.-J. Heo, C. G. Shin, H. Shim, J. W. Kim, Y. W. Jin and S. Lee, *J. Mater. Chem. C*, 2013, **1**, 5791.
- 94 M. G. Han, C. G. Shin, S.-J. Jeon, H. Shim, C.-J. Heo, H. Jin, J. W. Kim and S. Lee, *Adv. Mater.*, 2012, **24**, 6438–6444.
- 95 Y. Luo, J. Zhang, A. Sun, C. Chu, S. Zhou, J. Guo, T. Chen and G. Xu, *J. Mater. Chem. C*, 2014, **2**, 1990–1994.

- 96 I. Lee, D. Kim, J. Kal, H. Baek, D. Kwak, D. Go, E. Kim, C. Kang, J. Chung, Y. Jang, S. Ji, J. Joo and Y. Kang, *Adv. Mater.*, 2010, **22**, 4973–7.
- 97 M. Trau, D. a. Saville and I. a. Aksay, *Science*, 1996, **272**, 706–709.
- 98 M. Trau, D. Saville and I. Aksay, *Langmuir*, 1997, **7463**, 6375–6381.
- 5 99 T. Gong, D. Wu and D. Marr, *Langmuir*, 2003, **19**, 5967–5970.
- 100 H. Shim, J. Lim, C. Gyun Shin, S.-J. Jeon, M. Gyu Han and J.-K. Lee, *Appl. Phys. Lett.*, 2012, **100**, 063113.
- 101 C. Jin, X. Meng, B. Cheng, Z. Li and D. Zhang, *Phys. Rev. B*, 2001, **63**, 195107.
- 102 P. N. Pusey and W. van Meegen, *Nature*, 1986, **320**, 340–342.
- 10 103 P. N. Pusey, E. Zaccarelli, C. Valeriani, E. Sanz, W. C. K. Poon and M. E. Cates, *Philos. Trans. A. Math. Phys. Eng. Sci.*, 2009, **367**, 4993–5011.
- 104 K. Ueno, J. Sakamoto, Y. Takeoka and M. Watanabe, *J. Mater. Chem.*, 2009, **19**, 4778–4783.
- 105 H. Shim, C. Gyun Shin, C.-J. Heo, S.-J. Jeon, H. Jin, J. Woo Kim, Y. Jin, S. Lee, J. Lim, M. Gyu Han and J.-K. Lee, *Appl. Phys. Lett.*, 2014, **104**, 051104.
- 15 106 M. G. Han, C.-J. Heo, H. Shim, C. G. Shin, S.-J. Lim, J. W. Kim, Y. W. Jin and S. Lee, *Adv. Opt. Mater.*, 2014, **2**, 535–541.
- 107 J. Xia, Y. Ying and S. H. Foulger, *Adv. Mater.*, 2005, **17**, 2463–2467.
- 108 Y. Jiang, D. Xu, X. Li, C. Lin, W. Li, Q. An, C. Tao, H. Tang and G. Li, *J. Mater. Chem.*, 2012, **22**, 11943–11949.
- 20 109 S. Manakasettharn, T.-H. Hsu, J. A. Taylor and T. Krupenkin, *Opt. Mater. Express*, 2014, **4**, 681.
- 110 M. Shahinpoor and H.-J. Schneider, *Intelligent Materials*, The Royal Society of Chemistry, 2008.
- 111 M. Cianchetti, V. Mattoli, B. Mazzolai, C. Laschi and P. Dario, *Sensors Actuators, B Chem.*, 2009, **142**, 288–297.
- 25 112 Z. H. Fang, C. Punckt, E. Y. Leung, H. C. Schniepp and I. a Aksay, *Appl. Opt.*, 2010, **49**, 6689–6696.
- 113 Q. Zhao, A. Haines, D. Snoswell, C. Keplinger, R. Kaltseis, S. Bauer, I. Graz, R. Denk, P. Spahn, G. Hellmann and J. J. Baumberg, *Appl. Phys. Lett.*, 2012, **100**, 101902.

30



79x39mm (300 x 300 DPI)